Electronic Supplementary Material (ESI) for Journal of Materials Chemistry A.
This journal is © The Royal Society of Chemistry 2023

Electronic Supplementary Information

Porous $Ga_{0.25}Li_{6.25}La_3Zr_2O_{12}$ Frameworks by Gelcasting-Reaction Sintering for High-Performance Hybrid Quasi-Solid Lithium Metal Batteries

Ying Zhou [a], Ying Tian [a], Wen Wang *[a], Yu Zhou [a]

[a] Institute for Advanced Ceramics, School of Materials Science and Engineering, Harbin Institute of Technology, Harbin, 150001, P. R. China.

* Corresponding author: E-mail: wangwen@hit.edu.cn (W. Wang)

No. 92, Xidazhi Street, Nangang District, Harbin 150001, China

Tel. /Fax: +86 451 86414291

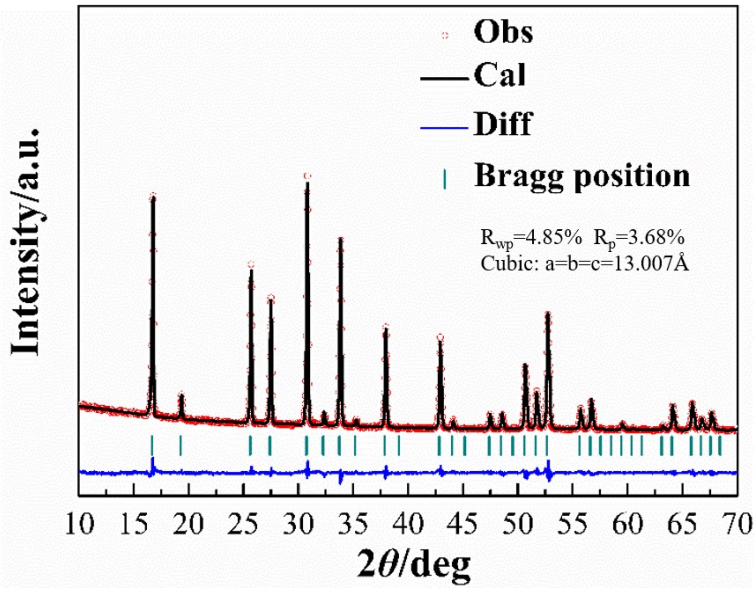

Fig. S1 The refined XRD patterns of the synthesized GLLZO powder

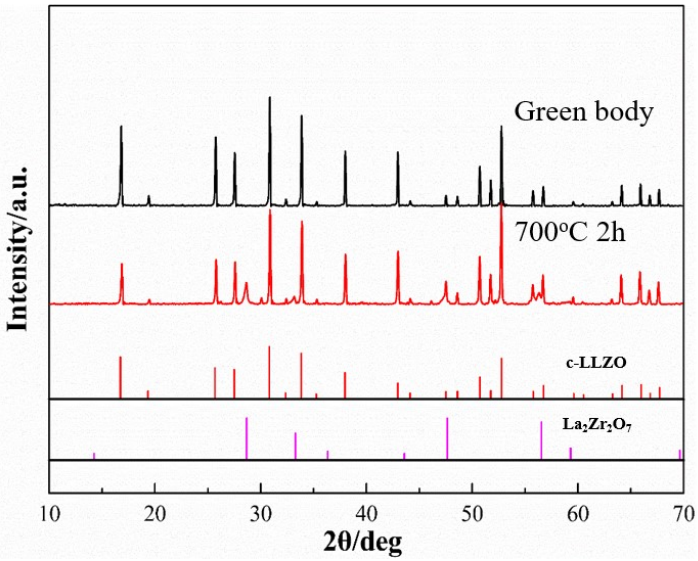

Fig. S2 XRD patterns of green body before and after de-bingding.

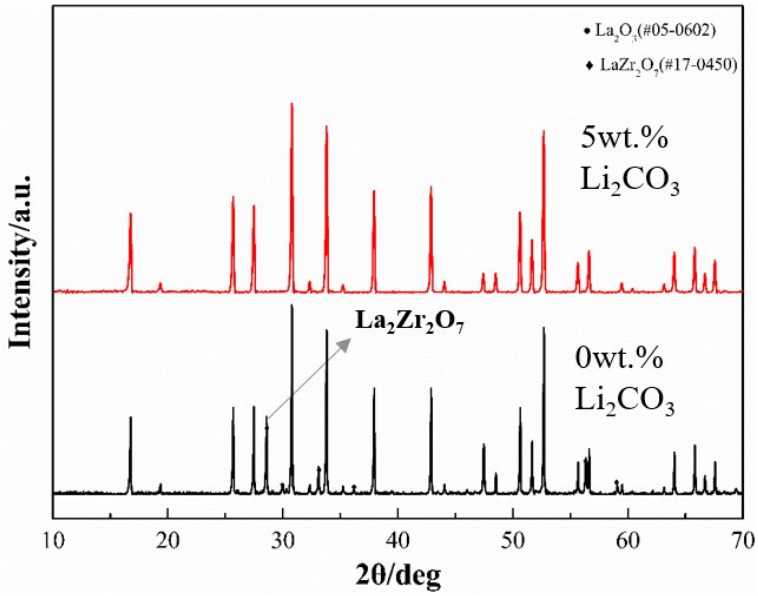

Fig. S3 XRD patterns of sintered LLZO frameworks prepared using 0wt.% Li_2CO_3 and 5wt.% Li_2CO_3.

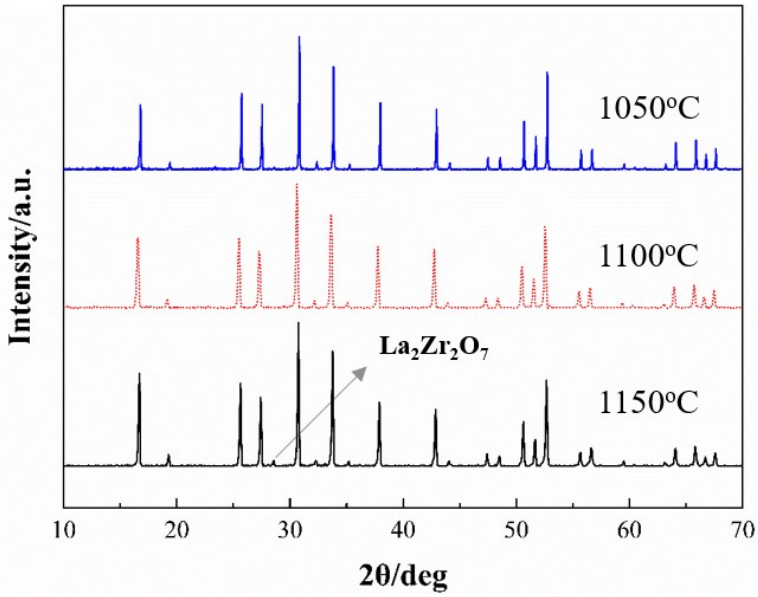

Fig. S4 XRD patterns of the LLZO framework obtained by using 5wt. % Li_2CO_3 at different sintering temperatures.

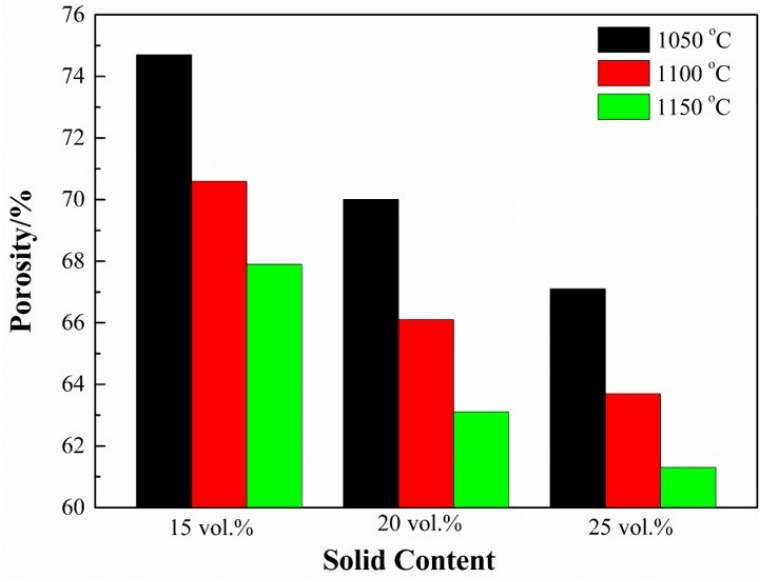

Fig. S5 Porosity of LLZO frameworks obtained by non-reaction sintering method at different temperatures with different solid content

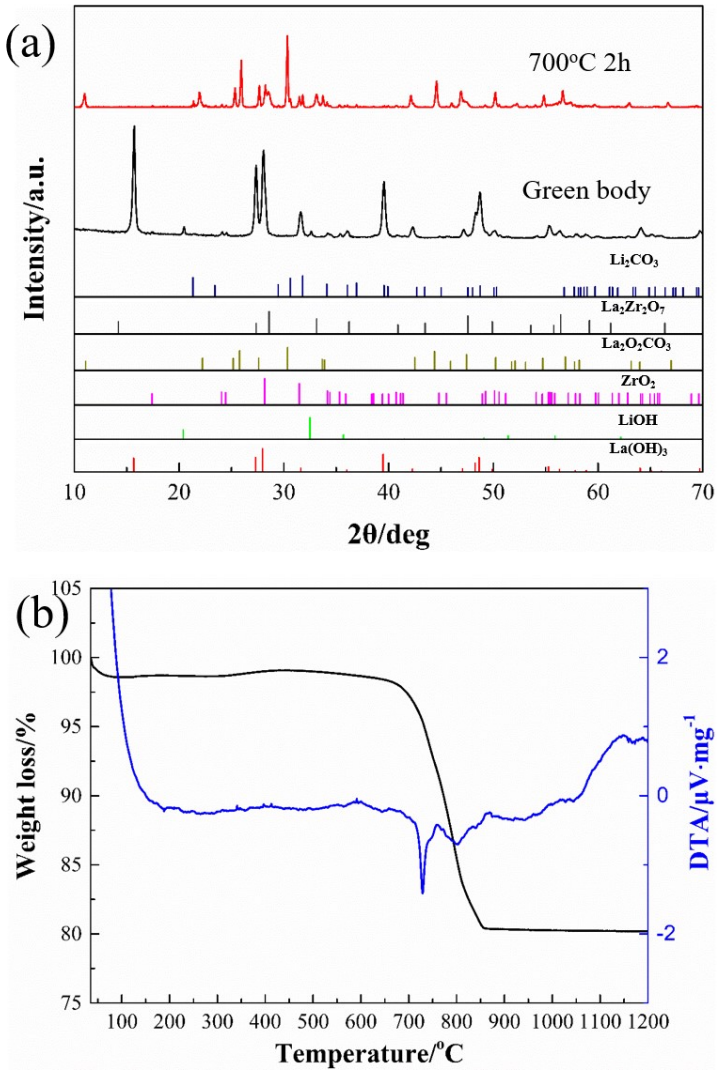

Fig. S6 a) XRD patterns of of green body before and after debingding. b) TG-DTA curves of the green body after debingding.

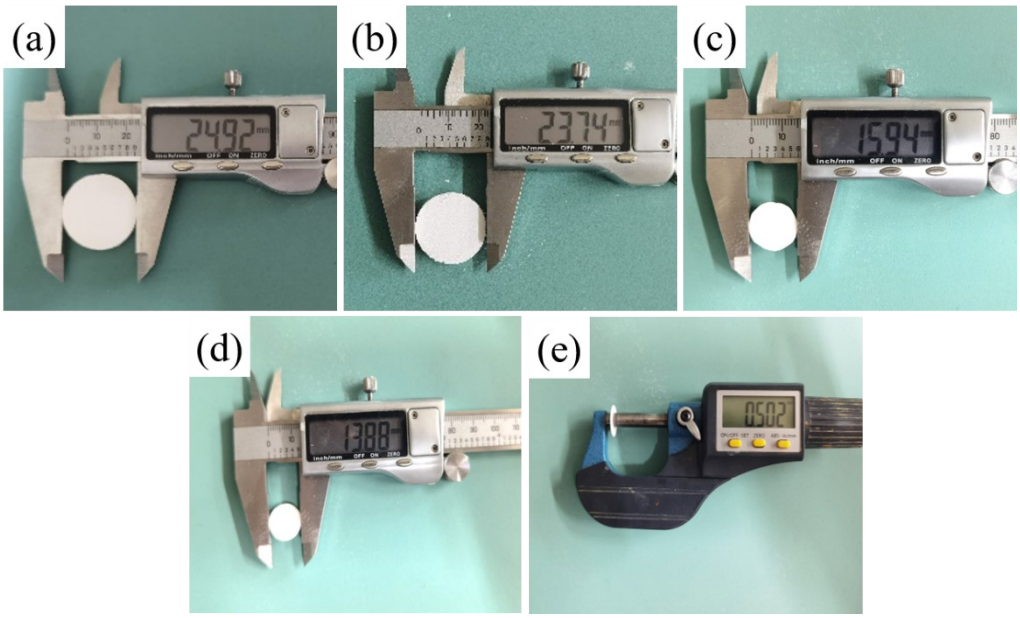

Fig. S7 The optical images of a) dried green body, b) green body after debinding, c) sintered LLZO framework at 1050 °C, d) and e) LLZO framework used to assemble battery

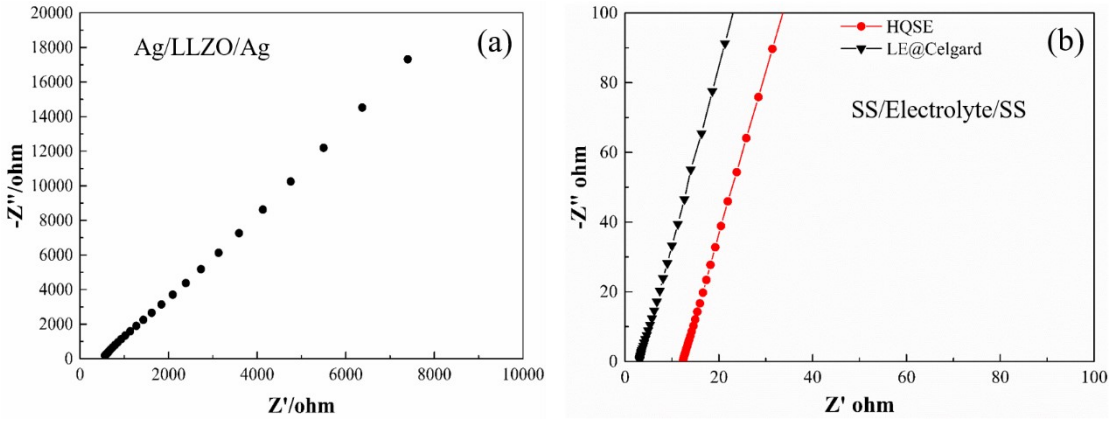

Fig. S8 Nyquits plots of a) DL, b) HQSE and LE@Celgard

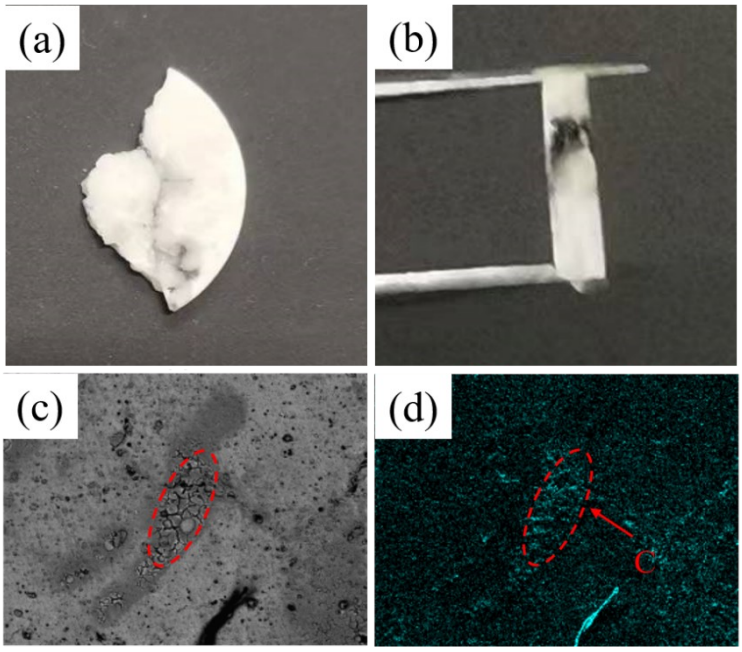

Fig. S9 a) Surface and b) cross-sectional digital photos of the DL collected after cell short circuit. c) Cross-sectional SEM image and d) EDS mappings of the DL collected after cell short circuit.

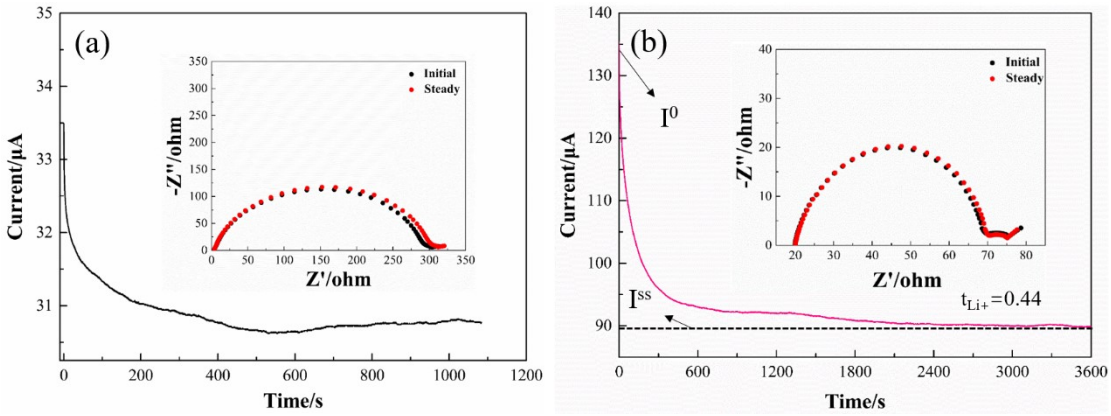

Fig. S10 The chronoamperometry profiles of symmetrical cells under a polarization voltage of 10 mV, and the EIS plots before and after the polarization. a) Li/LE@Celgard/Li, b) Li/HQSE/Li

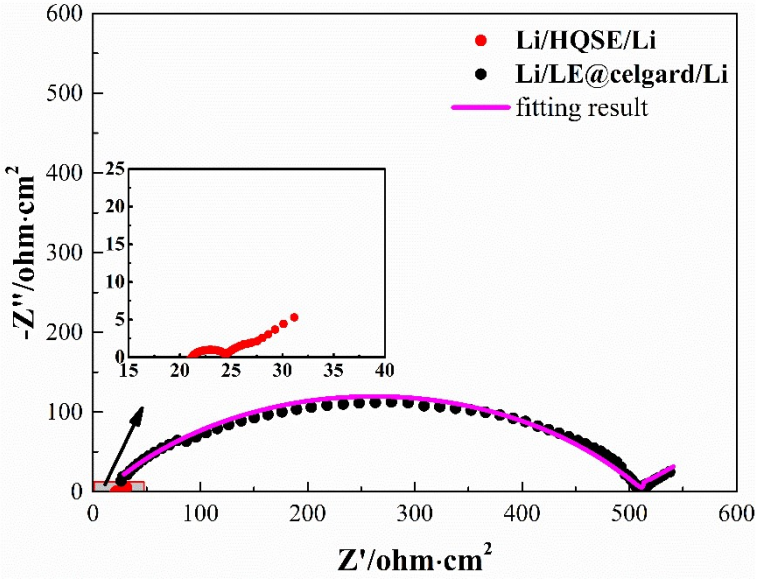

Fig. S11 EIS plots of Li/HQSE/Li and Li/LE@Celgard/Li symmetric cells after cycling.

Table S1 Composition of precursor slurry for non-reaction sintering

Samples	DMF (mL)	LLZO (g)	Li_2CO_3 (g)	AM (g)	MBAA (g)	AIBN (g)	solid content (Vol. %)
EX-1	15	13.63	0.4215	5	0.1667	1	15
EX-2	15	19.31	0.5972	5	0.1667	1	20
EX-3	15	25.75	0.7964	5	0.1667	1	25

Table S2 Composition of precursor slurry for reaction sintering

Samples	DMF (mL)	LLZO precursor. (g)	AM (g)	MBAA (g)	AIBN (g)	solid content (Vol. %)
IN-1	15	14.37	5	0.1667	1	22.5
IN-2	15	18.77	5	0.1667	1	27.5
IN-3	15	23.83	5	0.1667	1	32.5

Table S3 Main phase composition of the body before and after debinding

Samples	LiOH	La_2O_3	ZrO_2	-
Green body	LiOH	La_2O_3	ZrO_2	-
After debingding	Li_2CO_3	$La_2O_2CO_3$	ZrO_2	$La_2Zr_2O_7$

Table S4 The values of the ionic conductivity at 25°C

Samples	σ/Scm^{-1} (25°C)	σ/S^{-1} cm^{-1} K$^{-1/2}$ (25°C)	E_a/eV	T_0/K
LE@Celgard	0.82×10^{-3}	0.287	1.87×10^{-2}	161
HQSE	2.06×10^{-3}	0.550	1.10×10^{-2}	213

Table S5 Simulation results of Fig. 5c, d

Samples	Before cycling		After cycling	
	R_b ($\Omega\cdot cm^2$)	R_f ($\Omega\cdot cm^2$)	R_b ($\Omega\cdot cm^2$)	R_f ($\Omega\cdot cm^2$)
LFP/HQSE/Li	19.1	22.3	23.4	6.0
LFP/LE@Celgard/Li	3.7	51.6	11.0	137.1